Electronic Supplementary Material (ESI) for Faraday Discussions.

Electronic Supplementary Information:

Molecular dynamics simulations of carbon nanotube porins in lipid bilayers

Martin Vögele, Jürgen Köfinger, and Gerhard Hummer

Contents

1 Partial charges of armchair CNTs

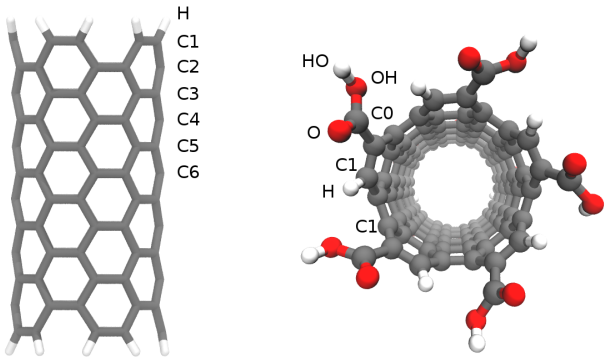

Fig. S1 Side view of a pristine armchair carbon nanotube and top view of a carboxylate-functionalized one with the respective atom names.

rings	H	C1	C2	C3	C4	C5	C6
6	0.134	-0.173	0.061	-0.022			
8	0.128	-0.151	0.033	-0.016	0.007		
10	0.129	-0.143	0.007	0.006	0.020	-0.018	
12	0.132	-0.161	0.047	-0.015	-0.019	0.043	-0.026
scheme	0.13	-0.16	0.03	0	0	0	0

Table S1 Partial charges of a non-functionalized armchair carbon nanotube with a ring size of 10 atoms: RESP charges for nanotubes with different sizes and the partial charge scheme we derived from this.

rings	HO	O	C1a	H	C1	C2	C3	C4	C5	C6
6	0.367	-0.514	0.227	0.188	-0.313	0.073	-0.050			
8	0.371	-0.529	0.241	0.168	-0.237	0.042	-0.089	0.041		
10	0.369	-0.533	0.251	0.185	-0.234	0.005	-0.049	0.051	-0.026	
12	0.370	-0.526	0.248	0.183	-0.283	0.052	-0.068	0.000	0.055	-0.035
scheme	0.37	-0.53	0.24	0.18	-0.28	0.01	0	0	0	0

Table S2 Partial charges of an OH-functionalized armchair carbon nanotube with a ring size of 10 atoms (every second H is replaced by OH): RESP charges for nanotubes with different sizes and the partial charge scheme we derived from this.

rings	O	O	C0	C1a	H	C1	C2	C3	C4	C5	C6
6	-0.849	-0.849	0.808	-0.084	0.183	-0.295	0.024	0.023			
8	-0.827	-0.828	0.762	-0.077	0.172	-0.226	0.024	-0.001	-0.045		
10	-0.809	-0.807	0.722	-0.080	0.159	-0.104	0.009	-0.027	0.003	0.009	
12	-0.841	-0.840	0.830	-0.093	0.223	-0.342	0.046	0.046	-0.090	0.021	0.019
scheme	-0.84	-0.84	0.83	-0.09	0.22	-0.34	0.03	0	0	0	0

Table S3 Partial charges of a COO^{-1}-functionalized armchair carbon nanotube with a ring size of 10 atoms (every second H is replaced by COO^{-}): RESP charges for nanotubes with different sizes and the partial charge scheme we derived from this.

rings	HO	OH	O	C0	C1a	H	C1	C2	C3	C4	C5	C6
6	0.436	-0.603	-0.535	0.725	-0.105	0.176	-0.148	0.035	-0.013			
8	0.441	-0.597	-0.528	0.685	-0.086	0.162	-0.113	0.031	0.001	-0.007		
10	0.453	-0.609	-0.547	0.695	-0.079	0.171	-0.129	0.029	0.003	-0.004	0.017	
12	0.441	-0.606	-0.545	0.705	-0.093	0.173	-0.121	0.038	-0.010	-0.004	0.021	-0.007
scheme	0.44	-0.60	-0.55	0.70	-0.1	0.17	-0.12	0.03	0	0	0	0

Table S4 Partial charges of a COOH-functionalized armchair carbon nanotube with a ring size of 10 atoms (every second H is replaced by COOH): RESP charges for nanotubes with different sizes and the partial charge scheme we derived from this.

2 Partial charges of zigzag CNTs

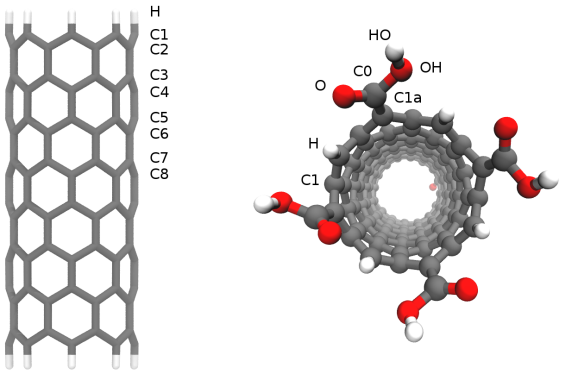

Fig. S2 Side view of a pristine zigzag carbon nanotube and top view of a carboxylate-functionalized one.

rings	H	C1	C2	C3	C4	C5	C6
2	0.165	-0.305	0.140				
4	0.168	-0.304	0.140	-0.001	-0.004		
6	0.167	-0.299	0.136	-0.009	0.013	-0.015	0.006
scheme	0.16	-0.30	0.14	0	0	0	0

Table S5 Partial charges of a non-functionalized zigzag carbon nanotube with a ring size of 8 atoms: RESP charges for nanotubes with different sizes and the partial charge scheme we derived from this.

rings	HO	O	C1a	H	C1	C2	C3	C4	C5	C6
2	0.306	-0.381	0.186	0.044	-0.046	-0.055				
4	0.312	-0.390	0.185	0.058	-0.094	-0.008	-0.055	0.027		
6	0.315	-0.399	0.212	0.065	-0.098	-0.023	-0.036	0.015	0.011	-0.014
scheme	0.31	-0.40	0.2	0.07	-0.10	-0.04	0	0	0	0

Table S6 Partial charges of an OH-functionalized zigzag carbon nanotube with a ring size of 8 atoms (every second H is replaced by OH): RESP charges for nanotubes with different sizes and the partial charge scheme we derived from this.

rings	O	O	C0	C1a	H	C1	C2	C3	C4	C5	C6
2	-0.873	-0.873	0.854	-0.277	0.300	-0.438	0.069				
4	-0.860	-0.860	0.877	-0.418	0.381	-0.555	0.027	0.109	-0.014		
6	-0.863	-0.863	0.903	-0.335	0.390	-0.435	0.084	0.118	-0.109	0.016	-0.032
scheme	-0.86	-0.86	0.91	-0.33	0.39	-0.43	0.09	0	0	0	0

Table S7 Partial charges of a COO^{-1}-functionalized zigzag carbon nanotube with a ring size of 8 atoms (every second H is replaced by COO^{-}): RESP charges for nanotubes with different sizes and the partial charge scheme we derived from this.

rings	HO	OH	O	C0	C1a	H	C1	C2	C3	C4	C5	C6
2	0.453	-0.603	-0.563	0.715	-0.098	0.155	-0.112	0.008				
4	0.458	-0.615	-0.582	0.728	-0.150	0.190	-0.148	0.046	0.024	-0.006		
6	0.458	-0.625	-0.589	0.718	-0.147	0.187	-0.136	-0.008	0.017	0.014	0.012	0.003
scheme	0.46	-0.63	-0.58	0.72	-0.14	0.19	-0.14	0.06	0	0	0	0

Table S8 Partial charges of a COOH-functionalized zigzag carbon nanotube with a ring size of 8 atoms (every second H is replaced by COOH): RESP charges for nanotubes with different sizes and the partial charge scheme we derived from this.

3 Details of simulation setup and parameters

3.1 Atomistic simulations

The systems were set up as follows: We started from the structure obtained from the CHARMM-GUI Membrane Builder[1–3]. This structure contains 200 lipids for the simulations containing one CNT and 288 lipids for the simulations with two or four CNTs. Five additional simulations of an armchair CNT of 4.5 nm length with COOH end groups in a POPC membrane were performed in different box widths to check for possible finite-size effects. The box height was chosen to obtain a water thickness (minimum water height on top and bottom of the system) of 2.5 nm. We placed the respective CNTs at the center of the simulation box and removed all lipids overlapping with the CNTs using VMD.[4] Periodic boundary conditions were applied, with the membrane in the *xy* plane.

All of the atomistic simulations were performed in Amber 14[5] and followed the same procedure. To remove steric clashes, a steepest descent energy minimization of 5.000 steps was performed followed by 5.000 more steps using the conjugate gradient method. The system was heated up through two sequential MD runs. In the first run (2500 steps), the temperature was increased linearly from 0 to 100 K and in the next one (50000 steps) from 100 to 303 K. In all simulations, a time step of 2 fs was used. Temperature was controlled via Langevin dynamics with a collision frequency of 1.0 ps^{-1}. Pressure was set to 1.0 bar via anisotropic pressure scaling using a Berendsen barostat[6] with a pressure relaxation time of 2 ps. The same settings were used in ten subsequent runs (250000 steps) at a constant temperature of 303 K in which the system dimensions were equilibrated. To obtain correct density fluctuations in the subsequent data-production runs, the pressure coupling was changed to a Monte Carlo barostat which performed volume change attempts after every 100 steps. The simulations were run for at least 150 ns each.

3.2 Coarse-grained simulations

We simulated CNTs of various length, diameter and rim functionalization (SP3, SNda, none) in a POPC membrane to investigate their tilting behavior and to compare the MARTINI and atomistic model. In addition, we simulated one CNT of length 4.5 nm with SNda end groups in 50:50 POPC/DOPC membrane patches of various widths to test for possible finite size-effects.

We set up MARTINI lipid membranes using `insane.py`[7] under periodic boundary conditions with an edge length of 15 nm, each containing one initially upright CNT. First, a steepest descent energy minimization was performed for at most 15000 steps in order to remove steric clashes of the simulation beads. Then the system was equilibrated for 20 ns in an NPT ensemble with a timestep of 10 fs. The temperature was kept constant at 300 K by using a velocity rescaling thermostat[8] with a time constant of 1 ns. Semiisotropic pressure coupling (1 bar) was achieved by a Berendsen barostat with a time constant of 3 ns. In the data production runs of 5.2 μs each, temperature coupling was achieved by the same thermostat as before and semiisotropic pressure coupling (1 bar) by a Parrinello-Rahman barostat ($\tau_p = 12$ ns). The timestep was set to 20 fs.

lipid type	funct. type	length [nm]	number lipids	number water mol.	box width [nm]	box height [nm]	sim. time [μs]
POPE	OH	4.50	186	7601	6.89 ± 0.07	9.43 ± 0.08	0.23
DOPC	OH	4.50	188	8946	7.57 ± 0.14	8.32 ± 0.05	0.22
DPPC	OH	4.50	187	8012	6.93 ± 0.07	10.15 ± 0.08	0.24
POPC	COO^-	4.00	188	8782	7.99 ± 0.09	8.65 ± 0.17	0.26
POPC	COO^-	4.50	188	8753	8.73 ± 0.09	8.86 ± 0.09	0.22
POPC	COO^-	5.00	188	8724	7.52 ± 0.18	8.74 ± 0.10	0.24
POPC	COOH	4.00	188	8791	7.57 ± 0.16	9.05 ± 0.13	0.23
POPC	COOH	4.50	188	8758	6.94 ± 0.02	8.92 ± 0.04	0.24
POPC	COOH	5.00	188	8732	7.03 ± 0.11	9.20 ± 0.06	0.23
POPC	none	4.00	188	8805	7.68 ± 0.12	8.83 ± 0.09	0.21
POPC	none	4.50	188	8785	8.03 ± 0.07	8.79 ± 0.08	0.24
POPC	none	5.00	188	8756	7.96 ± 0.10	8.76 ± 0.07	0.23
POPC	OH	4.00	188	8803	7.13 ± 0.10	8.92 ± 0.08	0.26
POPC	OH	4.50	188	8776	7.77 ± 0.09	8.97 ± 0.11	0.20
POPC	OH	5.00	188	8748	7.71 ± 0.19	9.01 ± 0.09	0.23

Table S9 Atomistic simulations with one armchair CNT.

lipid type	funct. type	length [nm]	number lipids	number water mol.	box width [nm]	box height [nm]	sim. time [μs]
POPC	COO^-	4.00	189	8799	7.39 ± 0.06	8.66 ± 0.07	0.21
POPC	COO^-	4.50	189	8757	7.89 ± 0.16	8.75 ± 0.14	0.23
POPC	COO^-	5.00	189	8733	8.59 ± 0.13	8.91 ± 0.11	0.22
POPC	COOH	4.00	189	8804	6.54 ± 0.11	8.99 ± 0.11	0.21
POPC	COOH	4.50	192	8805	8.01 ± 0.11	8.82 ± 0.06	0.22
POPC	COOH	5.00	189	8742	7.02 ± 0.07	8.97 ± 0.06	0.22
POPC	none	4.00	189	8818	7.91 ± 0.03	8.85 ± 0.03	0.20
POPC	none	4.50	189	8784	7.92 ± 0.09	8.75 ± 0.10	0.21
POPC	none	5.00	189	8761	7.26 ± 0.09	8.76 ± 0.13	0.22
POPC	OH	4.00	189	8812	6.95 ± 0.06	8.92 ± 0.09	0.22
POPC	OH	4.50	189	8777	6.83 ± 0.08	8.77 ± 0.13	0.21
POPC	OH	5.00	189	8756	8.31 ± 0.14	8.83 ± 0.10	0.22

Table S10 Atomistic simulations with one zigzag CNT.

lipid type	funct. type	length [nm]	number lipids	number water mol.	box width [nm]	box height [nm]	sim. time [μs]
POPC	COO^-	4.50	265	12442	9.17 ± 0.06	8.79 ± 0.07	0.16
POPC	COO^-	4.50	268	12447	8.42 ± 0.09	8.66 ± 0.05	0.16
POPC	COO^-	4.50	263	12433	7.73 ± 0.10	8.81 ± 0.08	0.17
POPC	COO^-	4.50	267	12446	9.07 ± 0.12	8.79 ± 0.06	0.16
POPC	COOH	4.50	265	12456	8.51 ± 0.07	8.84 ± 0.05	0.16
POPC	COOH	4.50	268	12468	8.95 ± 0.13	8.81 ± 0.07	0.17
POPC	COOH	4.50	263	12450	8.53 ± 0.07	8.87 ± 0.07	0.17
POPC	COOH	4.50	266	12467	9.55 ± 0.06	9.02 ± 0.04	0.17
POPC	none	4.50	265	12513	9.98 ± 0.16	8.96 ± 0.11	0.15
POPC	none	4.50	268	12507	8.88 ± 0.09	8.79 ± 0.05	0.16
POPC	none	4.50	263	12502	9.10 ± 0.07	9.05 ± 0.07	0.16
POPC	none	4.50	266	12512	9.16 ± 0.14	8.90 ± 0.06	0.16
POPC	OH	4.50	265	12498	8.73 ± 0.08	8.96 ± 0.06	0.14
POPC	OH	4.50	268	12494	9.78 ± 0.09	8.84 ± 0.09	0.15
POPC	OH	4.50	267	12488	9.10 ± 0.08	8.94 ± 0.05	0.14
POPC	OH	4.50	266	12494	8.47 ± 0.07	8.92 ± 0.09	0.17

Table S11 Atomistic simulations with two armchair CNTs.

lipid type	funct. type	length [nm]	number lipids	number water mol.	box width [nm]	box height [nm]	sim. time [μs]
POPC	COO^-	4.50	237	12280	9.09 ± 0.05	9.17 ± 0.05	0.16
POPC	COO^-	4.50	250	12295	8.36 ± 0.06	8.85 ± 0.06	0.17
POPC	COOH	4.50	237	12305	8.22 ± 0.07	9.44 ± 0.06	0.16
POPC	COOH	4.50	250	12337	8.64 ± 0.07	9.02 ± 0.07	0.17
POPC	none	4.50	237	12404	9.72 ± 0.11	9.36 ± 0.09	0.16
POPC	none	4.50	250	12407	8.94 ± 0.07	9.27 ± 0.07	0.15
POPC	OH	4.50	237	12370	8.66 ± 0.07	9.43 ± 0.07	0.15
POPC	OH	4.50	250	12382	8.56 ± 0.07	9.11 ± 0.06	0.15

Table S12 Atomistic simulations with four armchair CNTs.

lipid type	funct. type	length [nm]	number lipids	number water mol.	box width [nm]	box height [nm]	sim. time [μs]
POPC	COOH	5.00	153	6078	7.55 ± 0.09	8.20 ± 0.06	0.18
POPC	COOH	5.00	188	8732	7.03 ± 0.11	9.20 ± 0.06	0.23
POPC	COOH	5.00	277	12499	9.44 ± 0.06	8.77 ± 0.04	0.14
POPC	COOH	5.00	437	19579	11.64 ± 0.13	8.55 ± 0.05	0.16
POPC	COOH	5.00	785	34922	14.57 ± 0.10	8.51 ± 0.03	0.11

Table S13 Atomistic simulations for testing effects of the box size.

funct. type	diam. [nm]	length [nm]	number lipids	number water beads	box width [nm]	box height [nm]	sim. time [μs]
SNda	1.20	3.26	704	15848	15.06 ± 0.05	13.55 ± 0.09	8.40
SNda	1.20	4.07	704	15803	15.04 ± 0.05	13.56 ± 0.09	8.40
SNda	1.20	4.88	704	15775	15.04 ± 0.05	13.56 ± 0.09	8.40
SNda	1.20	5.70	704	15730	15.05 ± 0.05	13.51 ± 0.09	8.40
SNda	1.20	6.51	704	15697	15.07 ± 0.05	13.45 ± 0.09	8.40
SNda	1.80	3.26	704	15838	15.12 ± 0.05	13.44 ± 0.09	8.40
SNda	1.80	4.07	704	15780	15.09 ± 0.05	13.48 ± 0.09	8.40
SNda	1.80	4.88	704	15723	15.09 ± 0.05	13.41 ± 0.09	8.40
SNda	1.80	5.70	704	15662	15.10 ± 0.05	13.39 ± 0.09	8.40
SNda	1.80	6.51	704	15611	15.13 ± 0.05	13.30 ± 0.09	8.40
SNda	2.39	3.26	704	15834	15.19 ± 0.05	13.30 ± 0.09	8.40
SNda	2.39	4.07	704	15764	15.17 ± 0.05	13.33 ± 0.09	8.40
SNda	2.39	4.88	704	15682	15.15 ± 0.05	13.33 ± 0.09	8.40
SNda	2.39	5.70	704	15607	15.16 ± 0.05	13.31 ± 0.09	8.40
SNda	2.39	6.51	704	15541	15.19 ± 0.05	13.22 ± 0.09	8.40
SP3	1.20	3.26	704	15848	15.08 ± 0.05	13.48 ± 0.09	8.40
SP3	1.20	4.07	704	15805	15.05 ± 0.05	13.53 ± 0.09	8.40
SP3	1.20	4.88	704	15772	15.04 ± 0.05	13.53 ± 0.09	8.40
SP3	1.20	5.70	704	15732	15.05 ± 0.05	13.51 ± 0.09	8.40
SP3	1.20	6.51	704	15699	15.06 ± 0.05	13.46 ± 0.09	8.40
SP3	1.80	3.26	704	15839	15.14 ± 0.05	13.39 ± 0.09	8.40
SP3	1.80	4.07	704	15779	15.11 ± 0.05	13.44 ± 0.09	8.40
SP3	1.80	4.88	704	15728	15.10 ± 0.05	13.41 ± 0.09	8.40
SP3	1.80	5.70	704	15663	15.10 ± 0.05	13.37 ± 0.09	8.40
SP3	1.80	6.51	704	15611	15.12 ± 0.05	13.35 ± 0.09	8.40
SP3	2.39	3.26	704	15834	15.21 ± 0.05	13.31 ± 0.09	8.40
SP3	2.39	4.07	704	15764	15.18 ± 0.05	13.29 ± 0.09	8.40
SP3	2.39	4.88	704	15684	15.16 ± 0.05	13.32 ± 0.09	8.40
SP3	2.39	5.70	704	15606	15.16 ± 0.05	13.28 ± 0.09	8.40
SP3	2.39	6.51	704	15535	15.18 ± 0.05	13.22 ± 0.09	8.40
none	1.20	3.26	704	15848	15.04 ± 0.05	13.59 ± 0.09	8.40
none	1.20	4.07	704	15804	15.04 ± 0.05	13.54 ± 0.09	8.40
none	1.20	4.88	704	15774	15.05 ± 0.05	13.53 ± 0.09	8.40
none	1.20	5.70	704	15732	15.07 ± 0.05	13.47 ± 0.09	8.40
none	1.20	6.51	704	15699	15.08 ± 0.05	13.45 ± 0.09	8.40
none	1.80	3.26	704	15838	15.08 ± 0.05	13.50 ± 0.10	8.40
none	1.80	4.07	704	15782	15.09 ± 0.05	13.49 ± 0.09	8.40
none	1.80	4.88	704	15728	15.10 ± 0.05	13.42 ± 0.09	8.40
none	1.80	5.70	704	15665	15.11 ± 0.05	13.38 ± 0.10	8.40
none	1.80	6.51	704	15612	15.12 ± 0.05	13.35 ± 0.09	8.40
none	2.39	3.26	704	15834	15.17 ± 0.05	13.36 ± 0.09	8.40
none	2.39	4.07	704	15760	15.15 ± 0.05	13.36 ± 0.09	8.40
none	2.39	4.88	704	15684	15.16 ± 0.05	13.31 ± 0.09	8.40
none	2.39	5.70	704	15599	15.18 ± 0.05	13.23 ± 0.09	8.40
none	2.39	6.51	704	15535	15.21 ± 0.05	13.18 ± 0.09	8.40

Table S14 Coarse-grained simulations of various CNTs in POPC to study tilting behavior.

funct. type	diam. [nm]	length [nm]	number lipids	number water beads	box width [nm]	box height [nm]	sim. time [μs]
SNda	1.20	4.88	72	1813	6.97 ± 0.05	9.33 ± 0.13	2.00
SNda	1.20	4.88	160	3536	10.31 ± 0.05	8.76 ± 0.08	2.00
SNda	1.20	4.88	352	7698	15.23 ± 0.05	8.73 ± 0.06	2.00
SNda	1.20	4.88	672	13448	21.01 ± 0.05	8.36 ± 0.04	2.00
SNda	1.20	4.88	1018	20813	25.85 ± 0.05	8.45 ± 0.03	2.00
SNda	1.20	4.88	1512	29774	31.49 ± 0.05	8.30 ± 0.03	2.00
SNda	1.20	4.88	2698	52494	42.05 ± 0.05	8.25 ± 0.02	2.00
SNda	1.20	4.88	5920	117134	62.28 ± 0.05	8.32 ± 0.01	2.00
SNda	1.20	4.88	10600	207376	83.33 ± 0.05	8.28 ± 0.01	2.00

Table S15 Coarse-grained simulations of a CNT in POPC/DOPC to study box-size dependence.

4 Detailed results of the atomistic simulations

4.1 Radial distribution functions of lipid tails

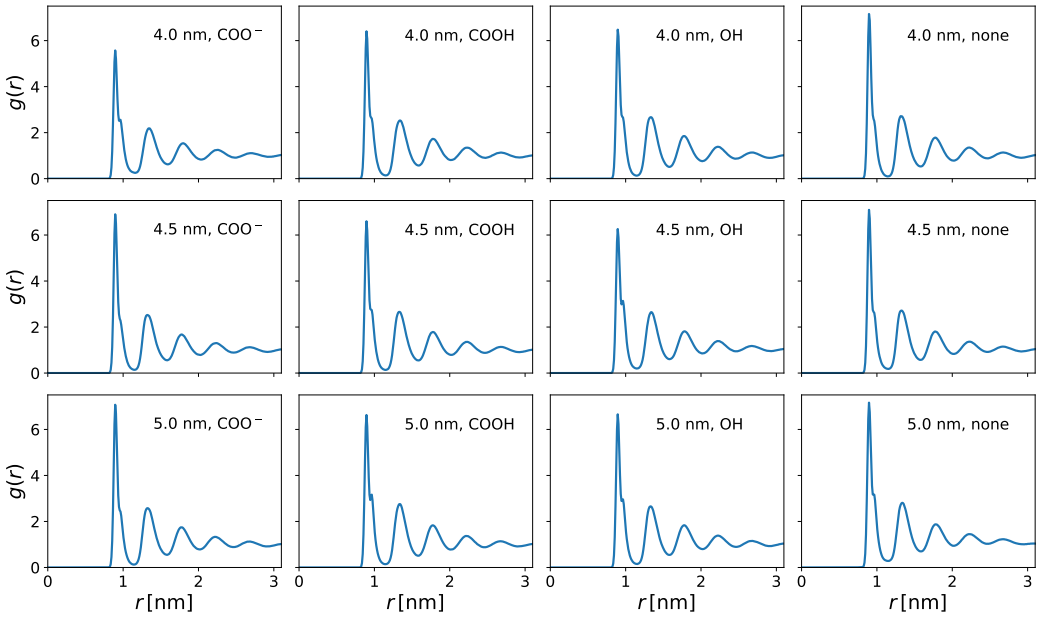

Fig. S3 RDF of the lipid-tail carbon atoms around the armchair carbon nanotubes

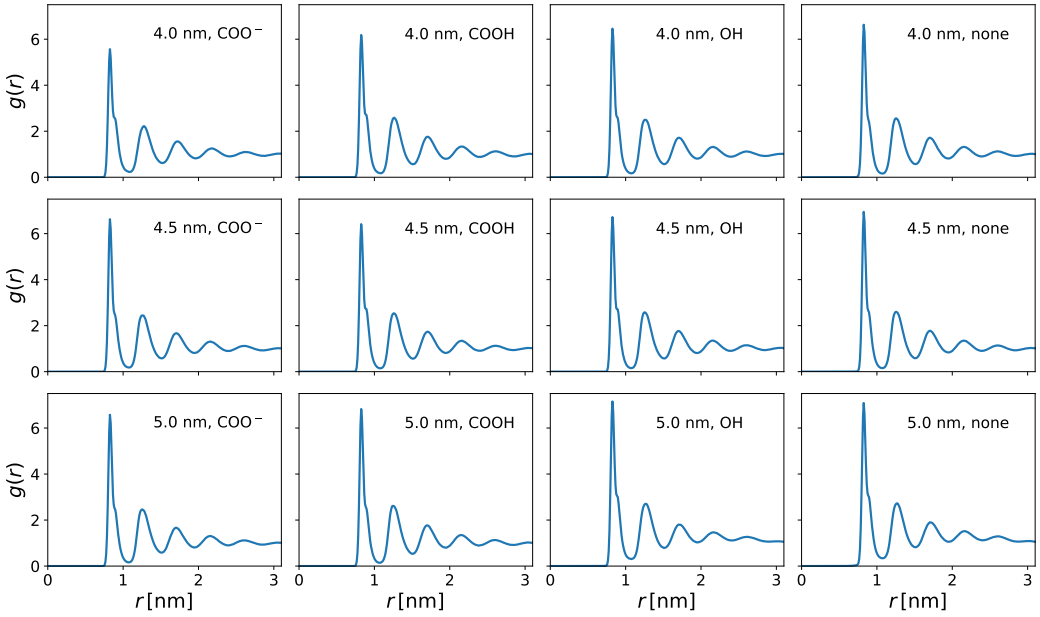

Fig. S4 RDF of the lipid-tail carbon atoms around the zigzag carbon nanotubes

4.2 Radial distribution functions of lipid headgroups

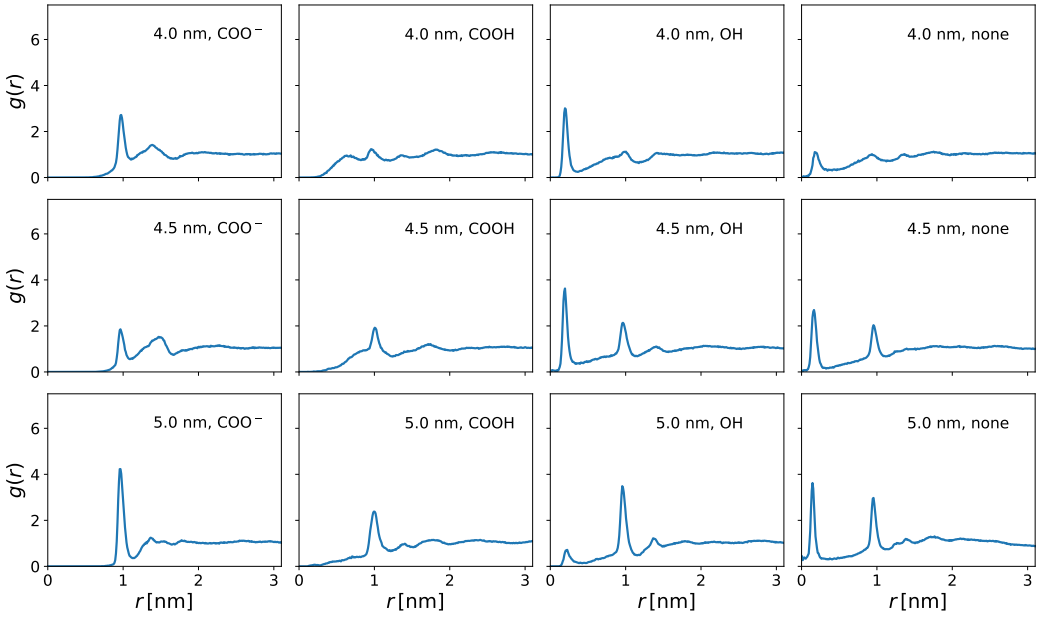

Fig. S5 RDF of the lipid-head nitrogen atoms around the armchair carbon nanotubes

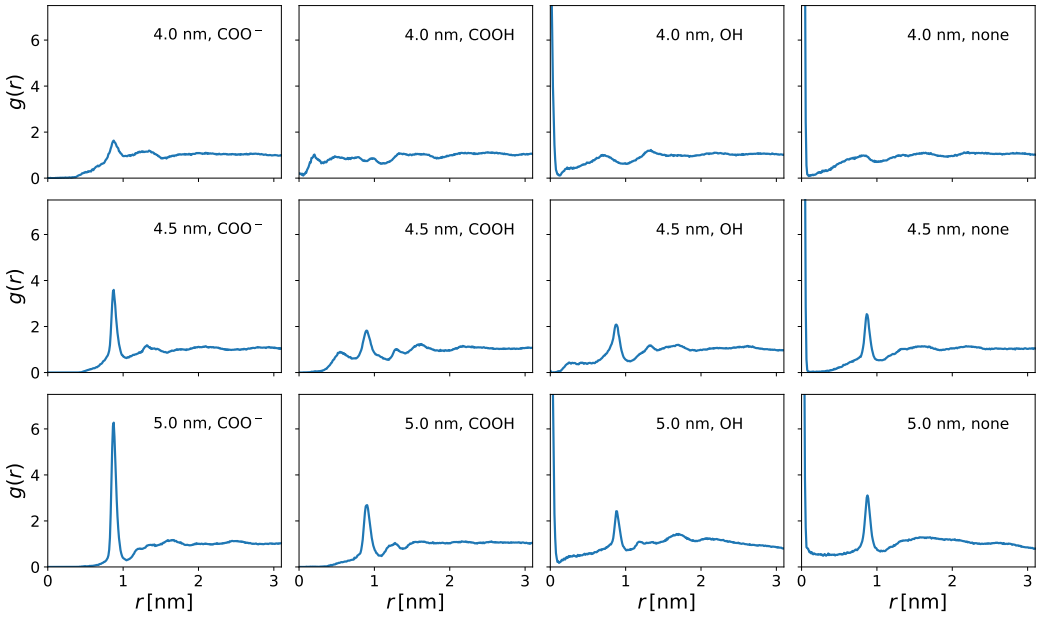

Fig. S6 RDF of the lipid-head nitrogen atoms around the zigzag carbon nanotubes

4.3 Order parameter

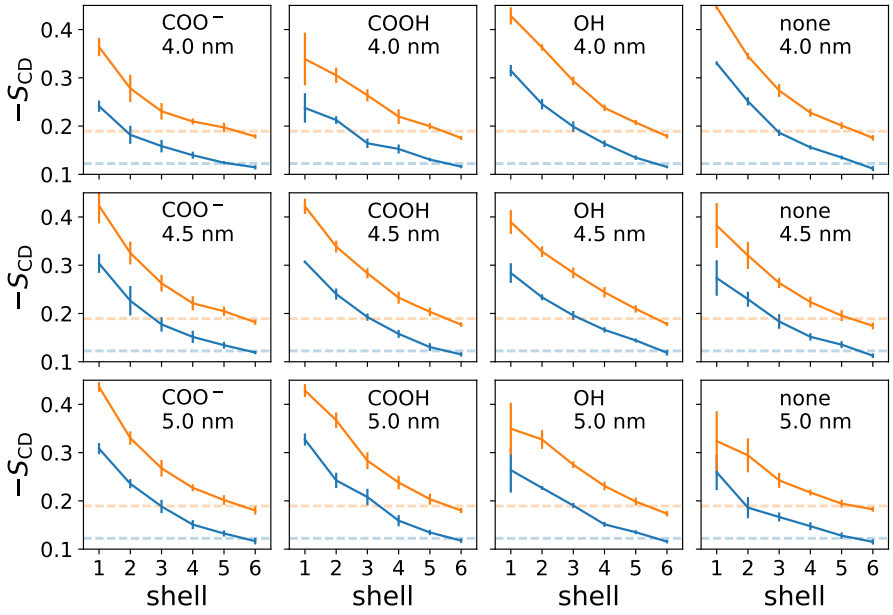

Fig. S7 Order parameter of the lipids around the armchair carbon nanotubes

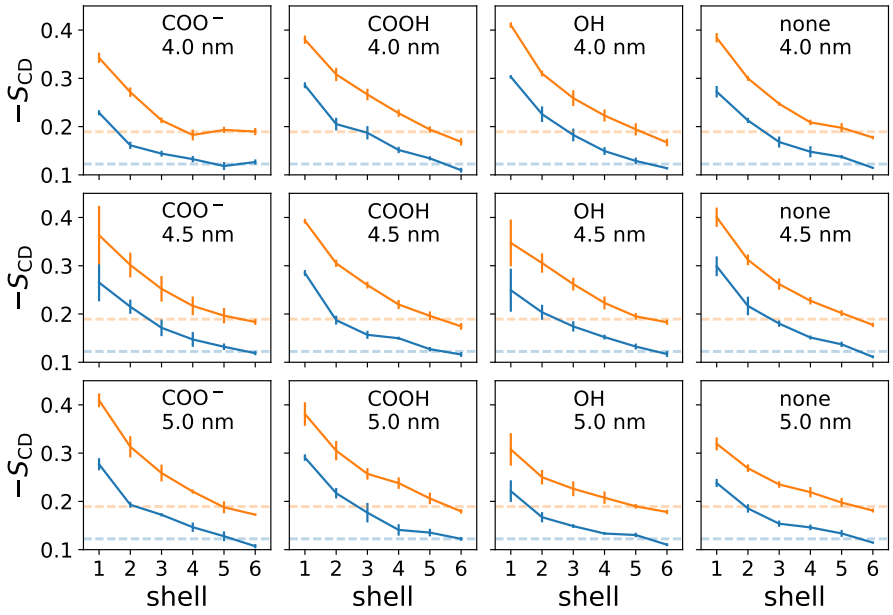

Fig. S8 Order parameter of the lipids around the zigzag carbon nanotubes

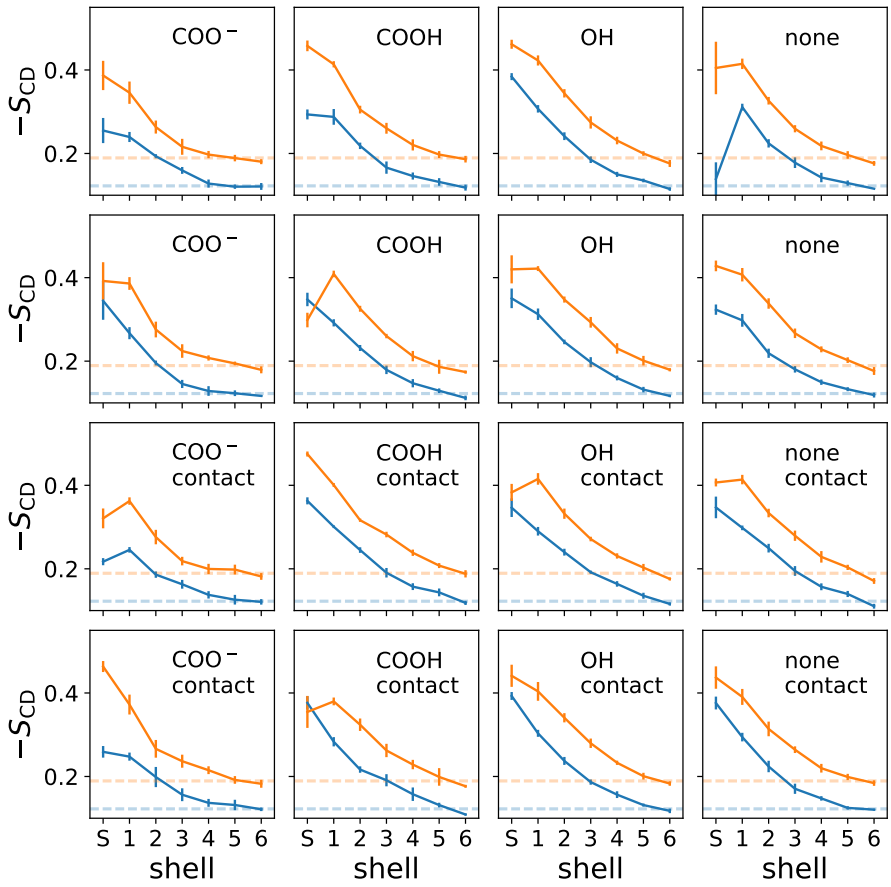

Fig. S9 Order parameter of the lipids in simulations of two armchair CNTs.

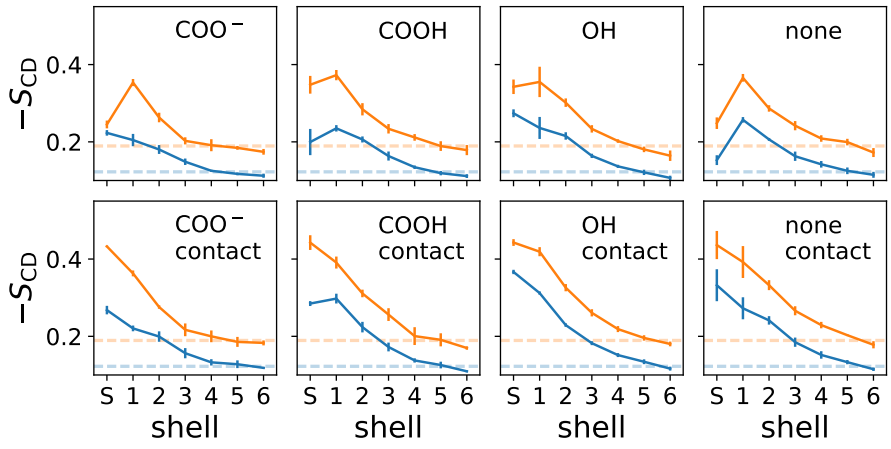

Fig. S10 Order parameter of the lipids in simulations of four armchair CNTs.

4.4 Water permeability

funct.	L	N_{wat}	D_n [ns^{-1}]	p_f [cm^3/s]
COO^-	4.0 nm	63.6 ± 2.3	29.6 ± 8.8	0.9 ± 0.3
	4.5 nm	70.0 ± 2.4	32.6 ± 9.7	1.0 ± 0.3
	5.0 nm	76.6 ± 2.5	37.3 ± 11.1	1.1 ± 0.3
COOH	4.0 nm	63.5 ± 2.4	26.9 ± 7.9	0.8 ± 0.2
	4.5 nm	71.3 ± 2.4	70.3 ± 20.7	2.1 ± 0.6
	5.0 nm	77.5 ± 2.7	49.4 ± 17.9	1.5 ± 0.5
OH	4.0 nm	59.7 ± 2.4	39.3 ± 12.2	1.2 ± 0.4
	4.5 nm	65.7 ± 2.4	27.5 ± 8.0	0.8 ± 0.2
	5.0 nm	73.5 ± 2.5	83.9 ± 25.8	2.5 ± 0.8
none	4.0 nm	57.3 ± 2.2	48.1 ± 13.9	1.4 ± 0.4
	4.5 nm	62.9 ± 2.5	41.8 ± 13.6	1.2 ± 0.4
	5.0 nm	68.4 ± 2.8	36.1 ± 13.2	1.1 ± 0.4

Table S16 Water transport properties of the armchair CNTs. Listed are the rim functionalization, the CNT length L, the average number N_{wat} of water molecules inside the CNT, the diffusion coefficient D_n of the net water permeation according to the collective diffusion model, and the water permeability p_f calculated from the respective D_n. Standard errors were estimated by block averaging using 12 blocks.

funct.	L	N_{wat}	D_n [ns^{-1}]	p_f [cm^3/s]
COO^-	4.0 nm	31.1 ± 2.1	3.2 ± 0.9	0.1 ± 0.1
	4.5 nm	36.8 ± 2.2	5.1 ± 1.5	0.2 ± 0.1
	5.0 nm	39.6 ± 2.4	5.2 ± 1.5	0.2 ± 0.1
COOH	4.0 nm	30.1 ± 2.3	14.5 ± 4.3	0.4 ± 0.1
	4.5 nm	34.8 ± 2.5	21.7 ± 6.2	0.6 ± 0.2
	5.0 nm	37.7 ± 2.6	26.9 ± 8.4	0.8 ± 0.2
OH	4.0 nm	28.3 ± 2.5	20.8 ± 6.7	0.6 ± 0.2
	4.5 nm	34.0 ± 2.5	32.5 ± 9.6	1.0 ± 0.3
	5.0 nm	35.6 ± 3.0	20.6 ± 8.3	0.6 ± 0.2
none	4.0 nm	25.0 ± 2.2	1.4 ± 0.2	0.0 ± 0.1
	4.5 nm	29.9 ± 2.5	2.1 ± 0.3	0.1 ± 0.1
	5.0 nm	33.5 ± 2.9	11.7 ± 5.4	0.3 ± 0.2

Table S17 Water transport properties of the zigzag CNTs. Listed are the rim functionalization, the CNT length L, the average number N_{wat} of water molecules inside the CNT, the diffusion coefficient D_n of the net water permeation according to the collective diffusion model, and the water permeability p_f calculated from the respective D_n. Standard errors were estimated by block averaging using 12 blocks.

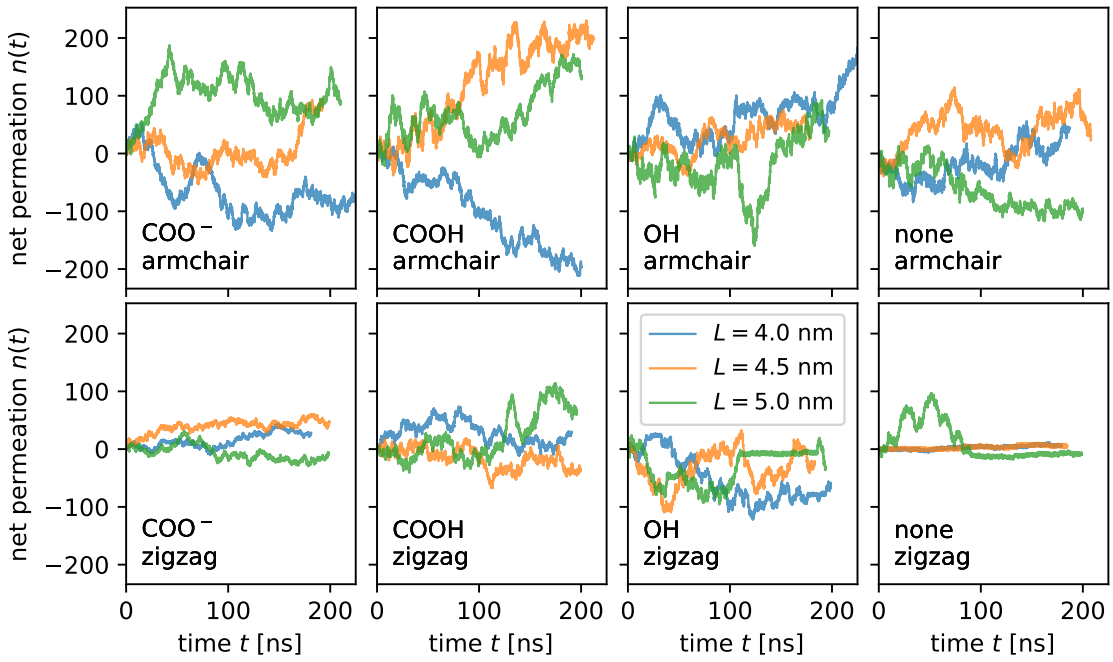

Fig. S11 Net water permeation $n(t)$ through the respective CNT porin over simulation time.

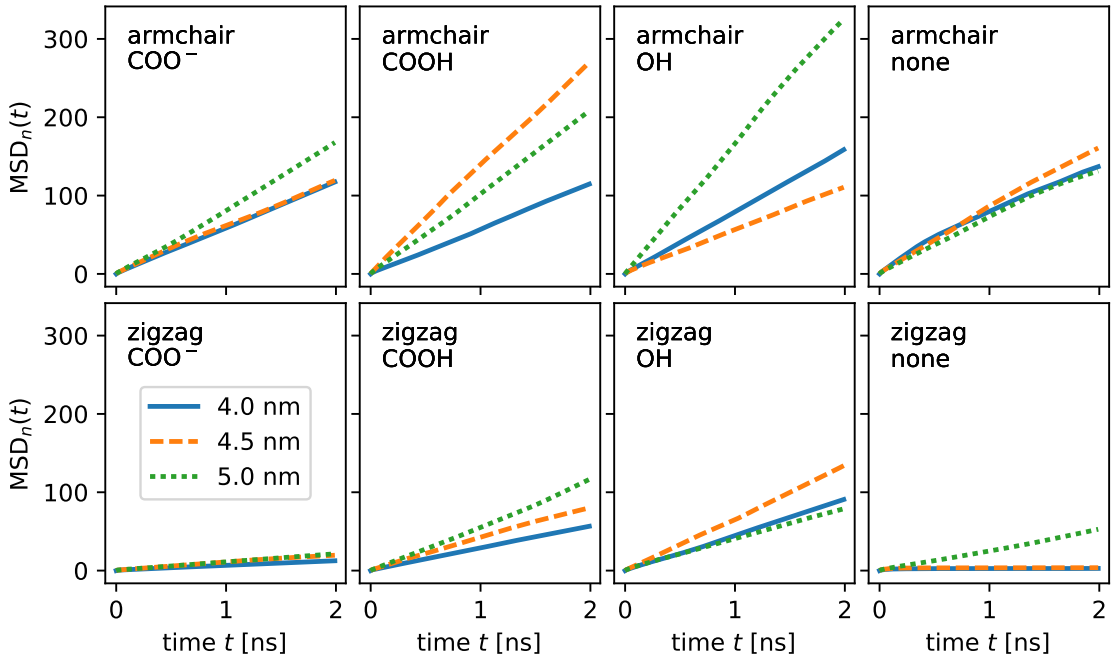

Fig. S12 Mean squared displacement (MSD) $\langle (n(t+\tau) - n(\tau))^2 \rangle_\tau$ during time t of the water net permeation $n(t)$, averaged over times τ along the MD trajectories.

4.5 Simulations of two and four CNTs

funct.	Repl.	initial contact	no init. contact
COO^-	A	contact	one layer
	B	contact	one layer
COOH	A	contact	one layer
	B	contact	two layers
OH	A	contact	one layer
	B	contact	one layer
none	A	contact	one layer
	B	contact	one layer

Table S18 Separation of two CNTs at the end of the simulation time (150 ns) after being prepared in initial contact (column 3) and separated (column 4). Each simulation was run twice (A and B). Column lists the number of lipid layers between the CNTs at the end of the simulations.

funct.	initial contact	no init. contact
COO^-	square	1,2,1,2 layers
	(slightly tilted)	1,2,1,2 layers
COOH	rhombus	1,1,2,2 layers
		1,2,2,2 layers
OH	rhombus	1,2,2,2 layers
		1,2,2,2 layers
none	rhombus	1,1,1,2 layers
		1,1,2,2 layers

Table S19 Separation of four CNTs at the end of the simulation time (150 ns) after being prepared in initial contact (column 2) and separated (column 3). Simulations with initial contact stayed in contact. Therefore, column 2 lists the resulting shape (Fig. S13 left). Simulations without initial contact remained approximately in a square (Fig. S13 right). Column 3 lists the number of layers of lipids between neighboring CNTs numbered along the sides of the square. For instance, "2,1,1,2" means that CNT pairs 1+2, 2+3, 3+4, and 1+4 are separated by 2, 1, 1, and 2 layers of lipids, respectively. The upper line gives values for the upper leaflet and the lower line for the lower leaflet.

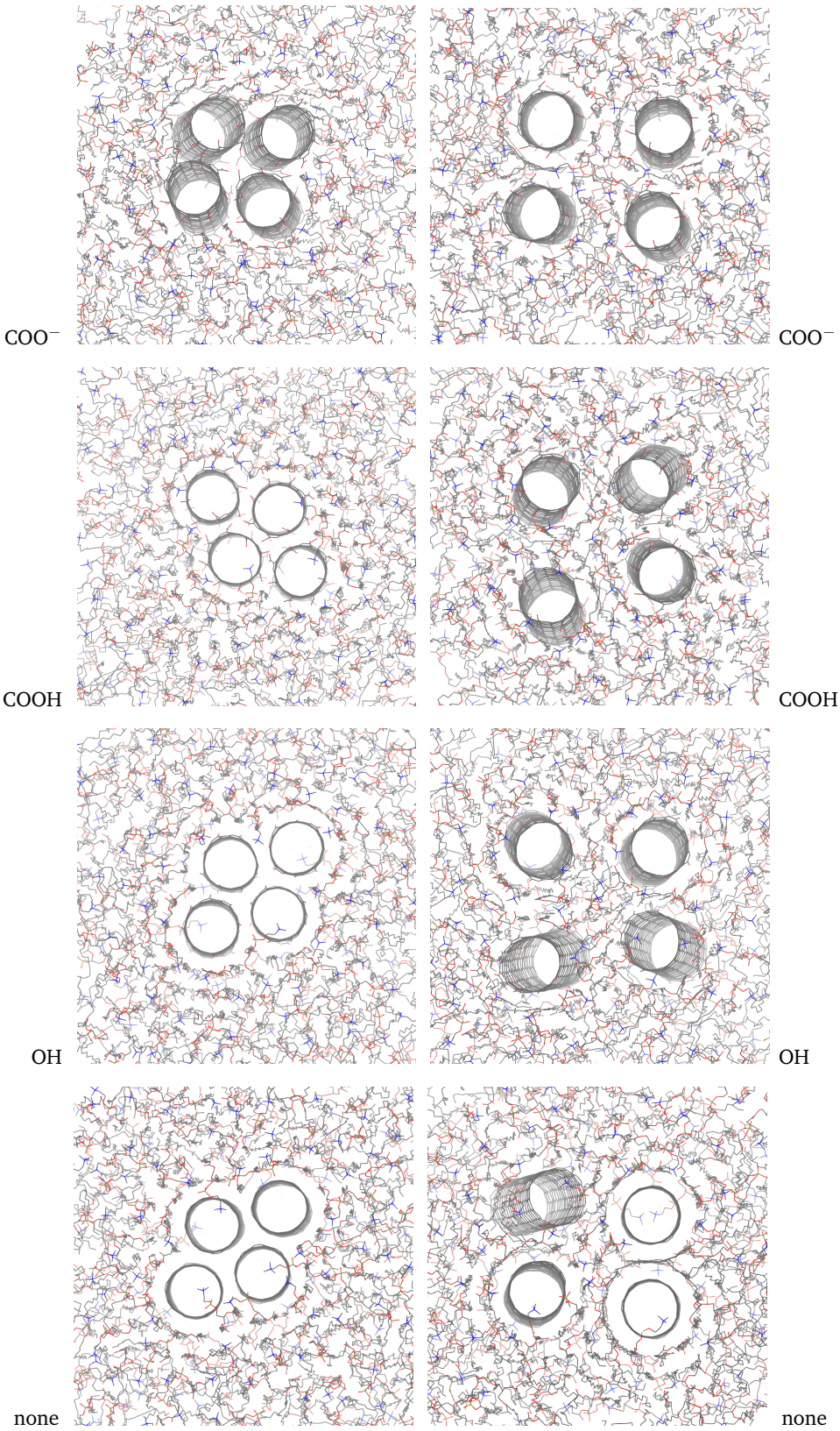

Fig. S13 Snapshots of atomistic simulations with four CNTs in a POPC membrane. The labels give the type of functional end group attached to the CNTs. Images on the left show simulations with initial contact and images on the right show simulations of initially separate CNTs. Snapshots were taken at the end of the simulation, i.e., after $\approx 150\,\mathrm{ns}$.

5 Effects of box size

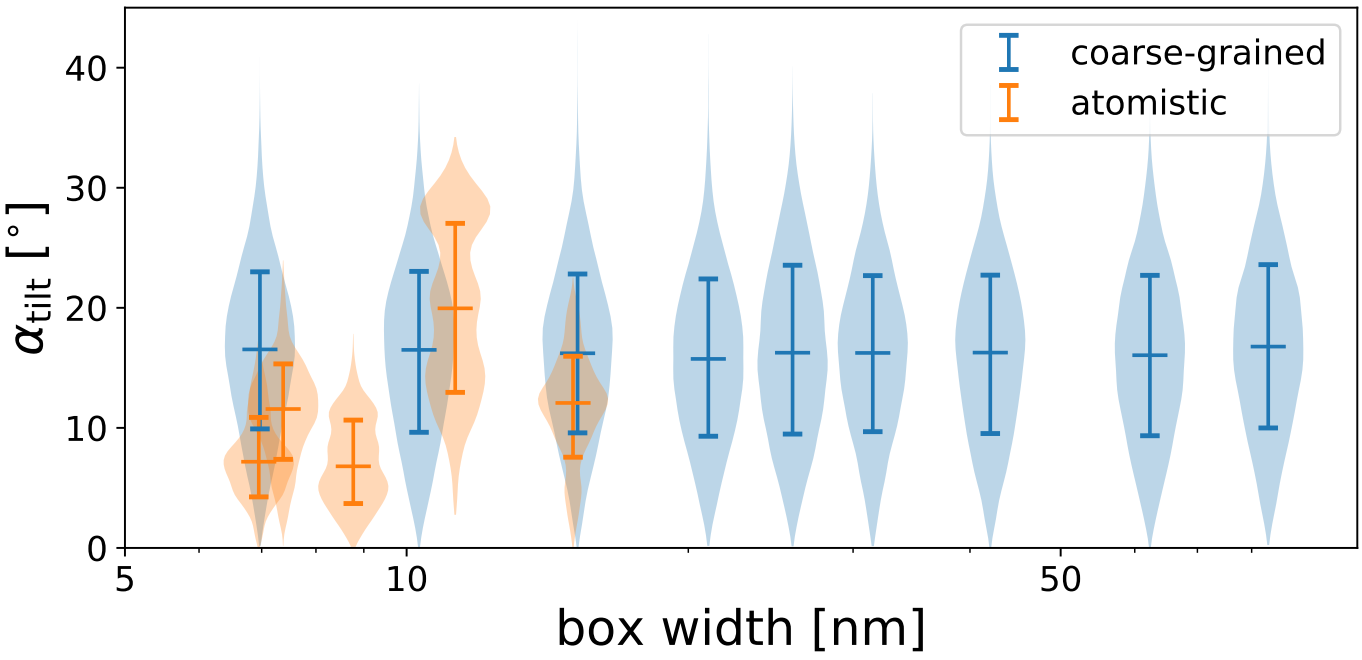

Fig. S14 Tilting angles of CNTs for atomistic and coarse-grained simulations in various box sizes. The atomistic simulations each contain a COOH-functionalized armchair CNT of 5 nm length in a POPC membrane ranging from 7 nm to 15 nm. The coarse-grained simulations contain a CNT of 4.5 nm length where rims were made of (weakly polar) SNda beads.

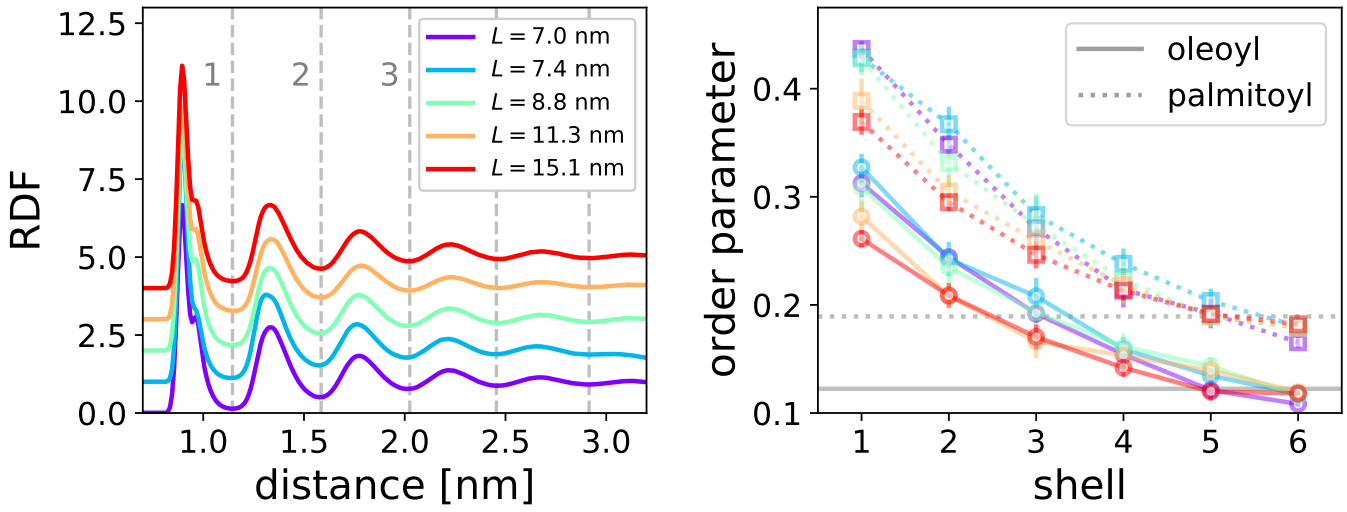

Fig. S15 Lipid structure in atomistic simulations of a CNT in different box sizes. (Left) Radial distribution function of lipid-tail carbon beads around the main axis of an armchair CNT of 4.5 nm length with COOH end groups in a POPC membrane. RDFs are shown for boxes of widths $L =$ 7.0, 7.4, 8.8, 11.3, and 15.1 nm (curves from bottom to top, shifted vertically in steps of 1.0). (Right) The lipid order parameter of oleoyl and palmitoyl tails in the distinct shells around the same coarse-grained CNT. Colors are assigned in the same way as in the left panel.

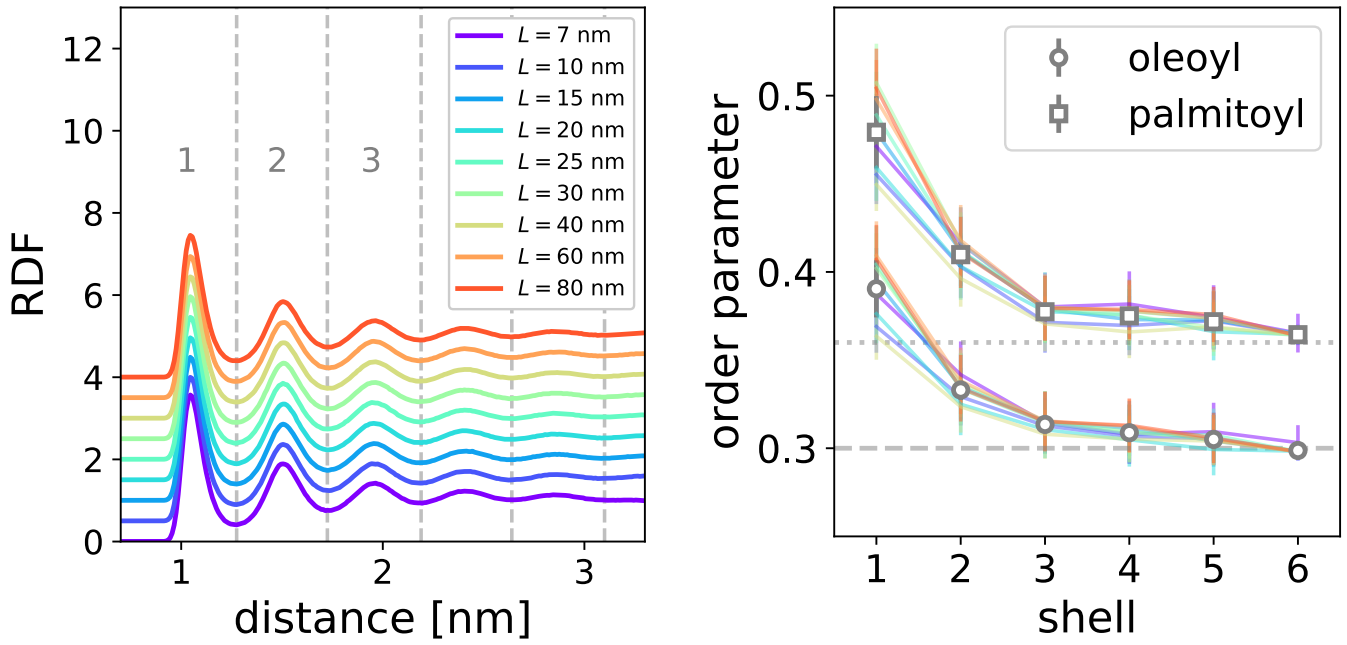

Fig. S16 Lipid structure in coarse grained simulations of a CNT in a POPC/DOPC membrane with different box sizes. (Left) Radial distribution function of lipid-tail carbon beads around the main axis of a coarse-grained CNT of 4.5 nm length with SNda end groups in a POPC/DOPC mixture. RDFs are shown for boxes of widths $L =$ 7, 10, 15, 20, 25, 30, 40, 60, and 80 nm (curves from bottom to top, shifted vertically in steps of 0.5). (Right) The lipid order parameter of oleoyl and palmitoyl tails in the distinct shells around the same coarse-grained CNT. Colors are assigned in the same way as in the left panel.

Notes and references

1 S. Jo, T. Kim, V. G. Iyer and W. Im, *J. Comput. Chem.*, 2008, **29**, 1859–1865.

2 S. Jo, J. B. Lim, J. B. Klauda and W. Im, *Biophys. J.*, 2009, **97**, 50–58.

3 E. L. Wu, X. Cheng, S. Jo, H. Rui, K. C. Song, E. M. Dávila-Contreras, Y. Qi, J. Lee, V. Monje-Galvan, R. M. Venable, J. B. Klauda and W. Im, *J. Comput. Chem.*, 2014, **35**, 1997–2004.

4 W. Humphrey, A. Dalke and K. Schulten, *J. Mol. Graph.*, 1996, **14**, 33–38.

5 D. Case, V. Babin, J. Berryman, R. Betz, Q. Cai, D. Cerutti, I. T.E. Cheatham, T. Darden, R.E.Duke, H. Gohlke, A. Goetz, S. Gusarov, N. Homeyer, P. Janowski, J. Kaus, I. Kolossváry, A. Kovalenko, T. Lee, S. LeGrand, T. Luchko, R. Luo, B. Madej, K. Merz, F. Paesani, D. Roe, A. Roitberg, C. Sagui, R. Salomon-Ferrer, G. Seabra, C. Simmerling, W. Smith, J. Swails, R. Walker, J. Wang, R. Wolf, X. Wu and P. Kollman, *AMBER 14*, 2014.

6 H. J. C. Berendsen, J. P. M. Postma, W. F. van Gunsteren, A. DiNola and J. R. Haak, *J. Chem. Phys.*, 1984, **81**, 3684–3690.

7 T. A. Wassenaar, H. I. Ingólfsson, R. A. Böckmann, D. P. Tieleman and S. J. Marrink, *J. Chem. Theory Comput.*, 2015, **11**, 2144–2155.

8 G. Bussi, D. Donadio and M. Parrinello, *J. Chem. Phys.*, 2007, **126**, —-.